Electronic Supplementary Material (ESI) for Environmental Science: Nano.
This journal is © The Royal Society of Chemistry 2016

Supporting Information (SI) on

X-ray absorption fine structure study of enhanced sequestration of U(VI) and Se(IV) by montmorillonite decorated zerovalent iron nanoparticles

Baowei Hu[1], Feng Ye[1], Xuemei Ren[4], Donglin Zhao[4,5], Guodong Sheng[1,2]*, Hui Li[1], Jingyuan Ma[3], Xiangke Wang[1,2,6], Yuying Huang[3]

1. College of Chemistry and Chemical Engineering, College of Life Science, or College of Medical Science, Shaoxing University, Zhejiang 312000, P.R. China

2. School of Chemistry and Environment, North China Electric Power University, Beijing 102206, P.R. China

3. Shanghai Synchrotron Radiation Facility (SSRF), Shanghai Institute of Applied Physics, Chinese Academy of Sciences, Shanghai 201204, P.R. China

4. Institute of Plasma Physics, Chinese Academy of Sciences, P.O. Box 1126, Hefei 230031, P.R. China

5. School of Materials and Chemical Engineering, Anhui University of Architecture, Hefei 230601, P.R. China

6. NAAM Research Group, Faculty of Science, King Abdulaziz University, Jeddah 21589, Saudi Arabia

***Corresponding authors**: Tel.: +86 575 8834 1526; fax: +86 575 8834 1521.

College of Chemistry and Chemical Engineering, Shaoxing University, Zhejiang 312000, P.R. China. Email: gdsheng@usx.edu.cn (G. Sheng)

Baowei Hu, hbw@usx.edu.cn (B. Hu)

Feng Ye, yefengusx@163.com (F. Ye)

Xuemei Ren, renxm1985@163.com (X. Ren)

Donglin Zhao, zhaodlin@126.com (D. Zhao)

Guodong Sheng, gdsheng@usx.edu.cn (G. Sheng)

Hui Li, lihui@usx.edu.cn (H. Li)

Jingyuan Ma, majingyuan@sinap.ac.cn (J. Ma)

Xiangke Wang, xkwang@ipp.ac.cn or xkwang@ncepu.edu.cn (X. Wang)

Yuying Huang, huangyuying@sinap.ac.cn (Y. Huang)

Synthesis of the materials

The homoionic Na^+-saturated montmorillonite (Na-montmorillonite, Na-Mont) and Al-pillared montmorillonite (Al-montmorillonite, Al-Mont) were synthesized by a simple cation exchange procedure. Herein, the raw Ca-montmorillonite (Ca-Mont) without size fraction was directly used to synthesize these supports [1]. For Na-Mont, concretely, ~10.0 g of Ca-Mont was dispersed in ~150 mL of NaCl solution and shaken at ~200 rpm, ~25 ^{0}C for ~10 h, then the suspension was centrifuged and the supernatant was discarded. The collected sample was re-suspended in ~150 mL of NaCl solution, then shaken and centrifuged as above. Five times repetitions were done to ensure complete Na^+ saturation. Finally, the Na^+-saturated product was washed with de-ionized water until no Cl^- was detected in the filtrate [1]. Then, we used the

as-synthesized Na-Mont to synthesize Al-Mont support. First, the pillaring solution was prepared by adding NaOH into ~0.20 mol/L $AlCl_3$, until the molar ratio of $[OH^-]/[Al^{3+}]$ achieved to be ~2.0. Then the pillaring solution was slowly added into ~10.0 g of Na-Mont suspension under continuous stirring in a water bath, the formed product was centrifuged and the supernatant was discarded. Then, the product was washed with de-ionized water until no Cl^- was detected in the filtrate, and finally dried in an oven. Before utilization, Na-Mont and Al-Mont were mechanically ground to a size of less than 100 meshes, and activated at ~110 ^{0}C for 2 h [1-3].

The nanoscale zero valent iron (NZVI) was synthesized by a chemical reduction procedure [2-4]. In brief, ~0.15 mol/L $NaBH_4$ was slowly added into ~0.05 mol/L $FeSO_4 \cdot 7H_2O$ under continuous stirring. Then the solution was stirred for ~30 min under room temperature. The NZVI particles formed were settled and separated from the liquid phase by vacuum filtration using Whatman (blue band) filter papers. Then the formed NZVI was washed with ethanol for several times, and finally vacuum-dried. The NZVI/Na-Mont and NZVI/Al-Mont composites were synthesized by a similar procedure for the preparation of NZVI, except that, before the addition of $NaBH_4$, ~10.0 g of Na-Mont or Al-Mont were uniformly mixed with 300.0 mL of 0.055 mol/L $FeSO_4 \cdot 7H_2O$ solution under continuous stirring. The as-synthesized iron sources were stored in N_2 atmosphere to prevent atmospheric contamination and oxidation [4]. The iron contents of the different reactive materials, using the atom absorption spectra in a Shimadzu AA-6300 spectrophotometer, were measured to be 90.8 % for ZVI, 52.6 % for NZVI, 21.5 % for NZVI/Al-Mont, and 20.2 % for

NZVI/Na-Mont, respectively.

Macroscopic measurements

The macroscopic measurements for U(VI) and Se(IV) sequestration onto various iron sources were carried out in a 100-mL conical flask in a water bath incubator of ~20 ^{0}C under N_2 conditions by using batch experiments. Typically, each sample containing a certain amount of iron was added into the conical flask with 100 mL of U(VI) or Se(IV) solution, which was deoxygenated by N_2 stream, The conical flask was sealed with a stopper during the experiment. The reaction was carried out by putting the flask in a thermostatic shaker bath. At given time intervals, a series of samples were withdrawn and filtered through 0.22-μm membrane for determination of U(VI) or Se(IV) concentrations. The concentration of U(VI) was determined by the arsenazo(III) spectrophotometric method at the wavelength of 650 nm [2, 4]. The concentrations of Se(IV) were analyzed by using Hydride generation atomic absorption spectrometry (HG-AAS, (AA-6300 C, Shimadzu)) [3]. The removal of U(VI) or Se(IV) was calculated: removal(%)= $(C_0-C_t)/C_0\times100\%$.

The adsorption isotherms of U(VI) or Se(IV) on Na-Mont and Al-Mont were determined. U(VI) or Se(IV) solution at various initial concentrations was mixed with a certain amount of Na-Mont and Al-Mont. All batch experiments were carried out in a thermostatic shaker bath. After adsorption equilibrium, the suspension was centrifuged, the supernatant was filtered through 0.22-μm membrane for determination of U(VI) or Se(IV) concentration. The adsorbed amounts (q_e(mg/g)) of

U(VI) or Se(IV) on Na-Mont and Al-Mont were calculated from the difference between initial (C_0(mg/L)) and equilibrium (C_e(mg/L)) concentration according to the equation, $q = \frac{(C_0 - C_e) \times V}{m}$, where V is the total volume of suspension (mL), and m is adsorbent mass (g).

Characterization methods

Scanning electron microscopy (SEM) images were obtained on a JSM-6360LV microscope instrument. Transmission electron microscope (TEM) images were obtained in a JEM-1010 instrument using an accelerating voltage of 80 kV. X-ray diffraction (XRD) measurement was performed with a Rigaku D/MAX-2500 system using Cu Ka radiation at 0.1542 nm. The zeta potential was measured by nano-ZS model (Malvern) zetasizer instrument. XPS spectra were collected using a Thermo ESCALAB 250 with a monochromatized Al Kα X-ray source (hν = 1486.6 eV) operated at a power of 150 W and a constant pass energy of 20 eV for the analyzer. The binding energies of the photoelectrons were corrected by C 1s peak at 284.8 eV. The Brunauer–Emmett–Teller (BET) specific surface areas were obtained from nitrogen adsorption data at 77 K in a Micromeritics ASAP 2020 system. The solution pH was measured with a pH meter (PHS-2C, China). U L_3-edge X-ray absorption fine structure (XAFS) spectra at ~17166 eV and Se K-edge XAFS spectra at ~12684.5 eV for the solid products were recorded at the beamline 14W in Shanghai Synchrotron Radiation Facility (SSRF, China). The electron beam energy was 3.5 GeV and the mean stored current was 300 mA. All spectra were collected in fluorescence mode

using a multi-element pixel high purity Ge solid-state detector. Scans were collected in triplicate and averaged to improve the signal-to-noise ratio. Analysis of extended X-ray absorption fine structure (EXAFS) and X-ray absorption near edge structure (XANES) was performed using Athena and Artemis interfaces of the IFFEFIT software [5, 6]. First, the averaged spectra were normalized with respect to E_0 determined from the second derivative of the raw spectra, and then the total atomic cross-sectional absorption was set to unity. A low-order polynomial function was fit to the pre-edge region and the post-edge region. Next, the data were converted from E-space to *k*-space and weighted by k^3 to compensate for dampening of the XAFS amplitude with increasing *k* space. Fourier transformation was then performed over the *k* range of 2.0-10.0 $Å^{-1}$ using the Kaiser-Bessel window function to obtain the radial structural functions (RSFs). Final fitting of the spectra was done on Fourier transformed k^3-weighted spectra in R-space. Theoretical EXAFS amplitude and phase functions for Se-O, Se-Se, Se-Fe and U-O, U-U, U-Fe and U-Al/Si single scattering paths were generated by FEFF 7.0 [7]. Fitted parameters such as interatomic distance (R), coordination number (N) and Debye-Waller factor (σ^2) were first established with reasonable guesses and were fitted in R-space.

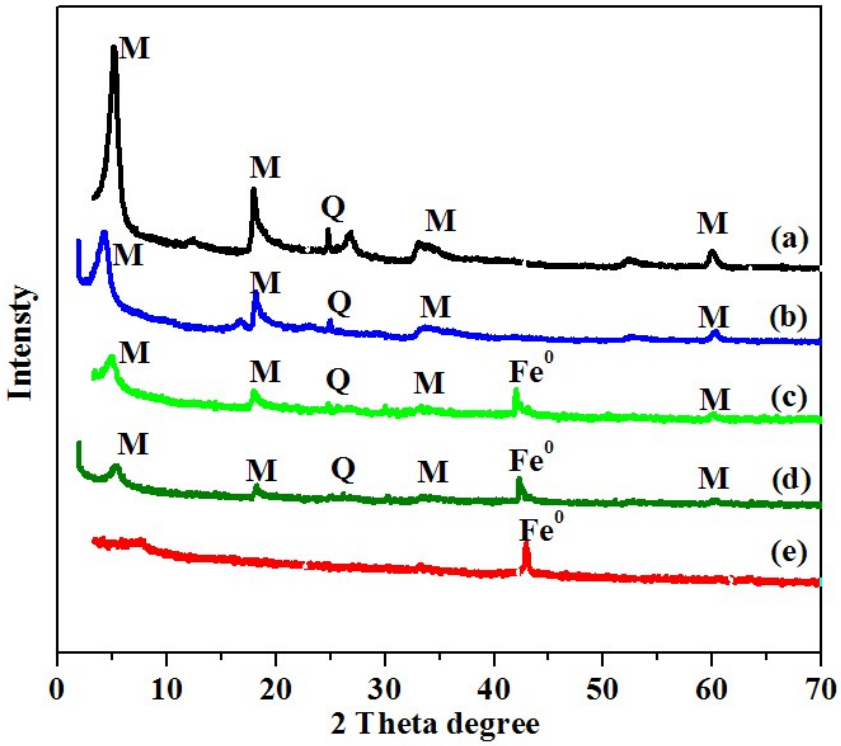

FIGURE S1. The XRD patterns of (a) Na-Mont, (b) Al-Mont, (c) NZVI/Na-Mont, (d) NZVI/Al-Mont, and (e) NZVI, M: montmorillonite, Q: quartz.

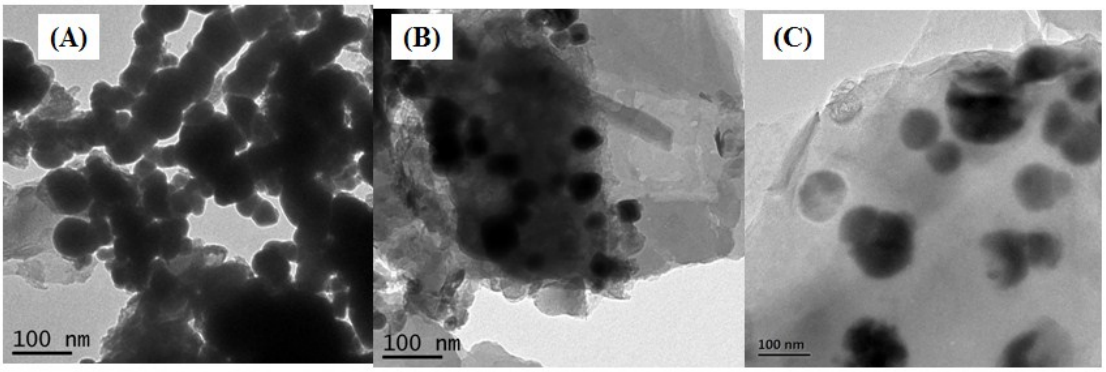

FIGURE S2. TEM images of (A) NZVI, (B) NZVI/Na-Mont, and (C) NZVI/Al-Mont.

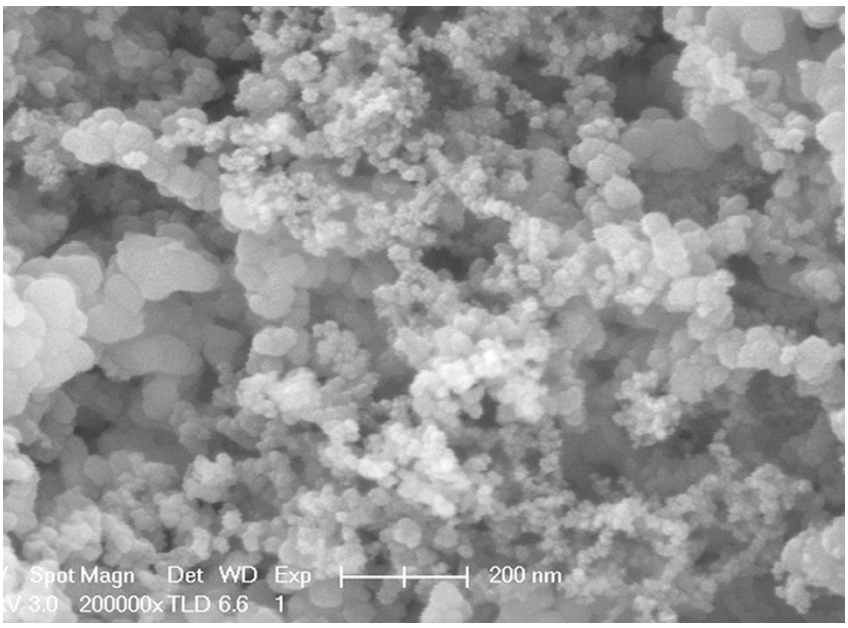

FIGURE S3. The SEM image of NZVI.

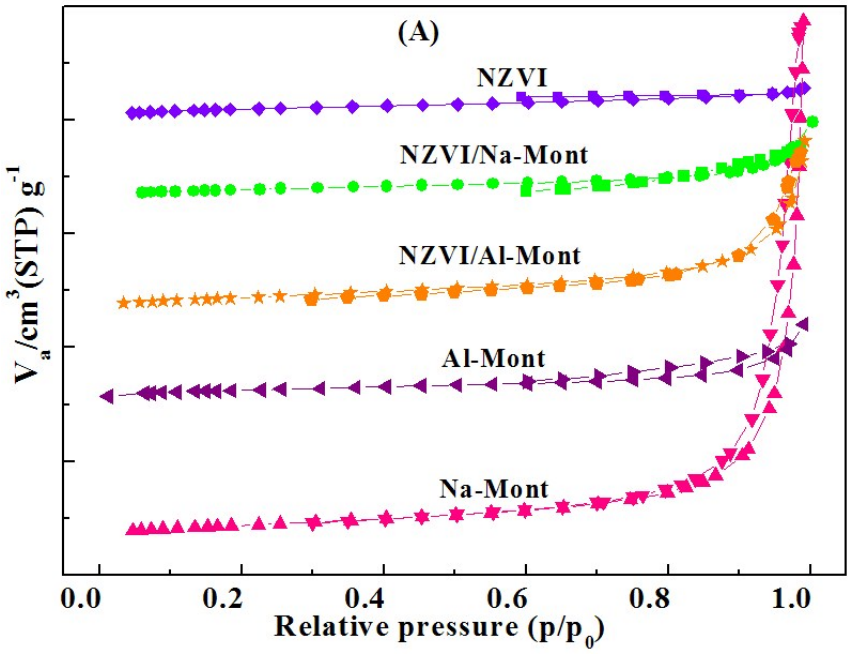

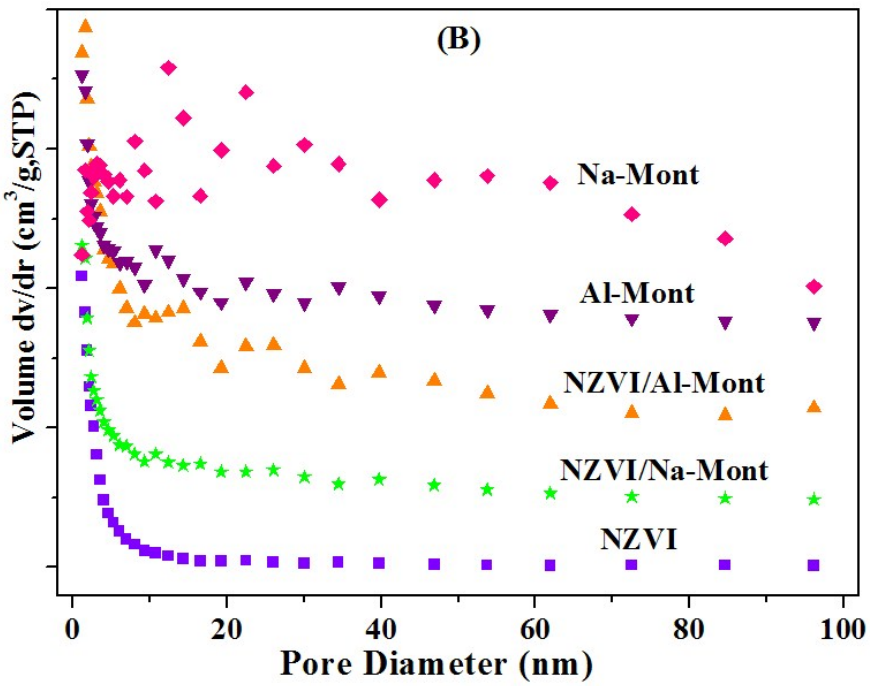

FIGURE S4. N_2 adsorption-desorption isothermal (A) and corresponding BJH pore-size distribution curve (B) of Na-Mont, Al-Mont, NZVI/Na-Mont, NZVI/Al-Mont, and NZVI, the pore-size distribution was calculated from the desorption branch of the isotherm.

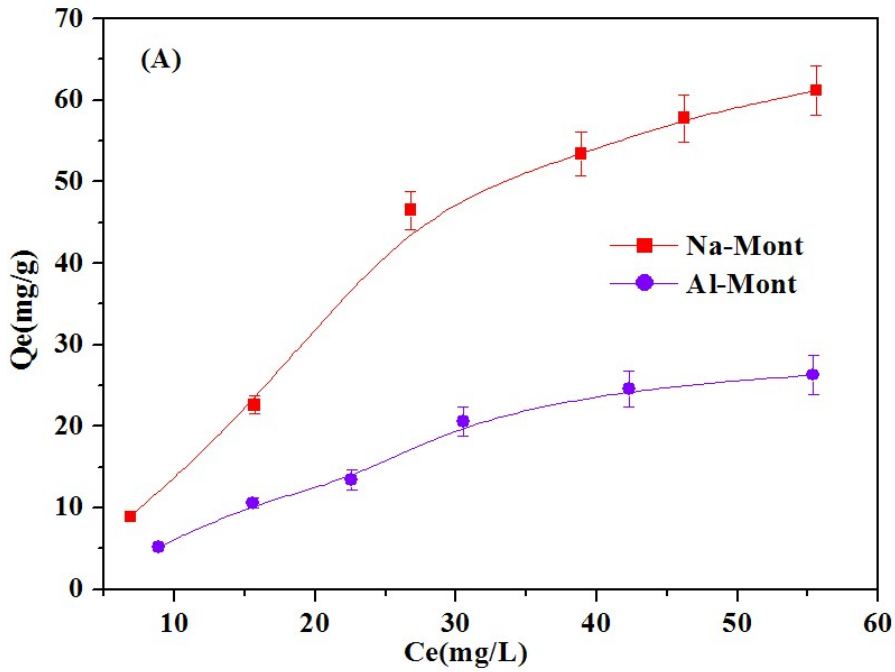

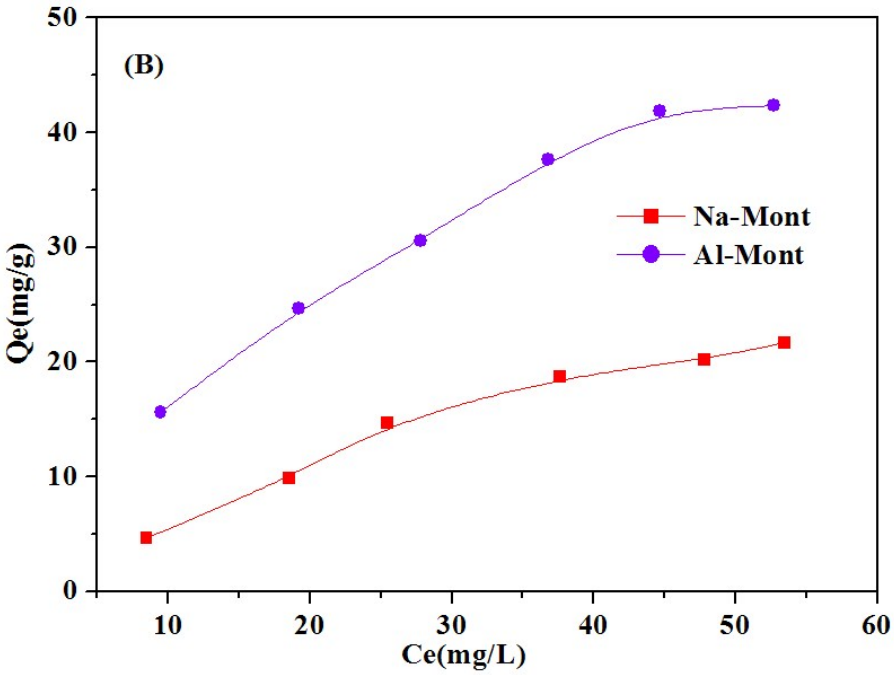

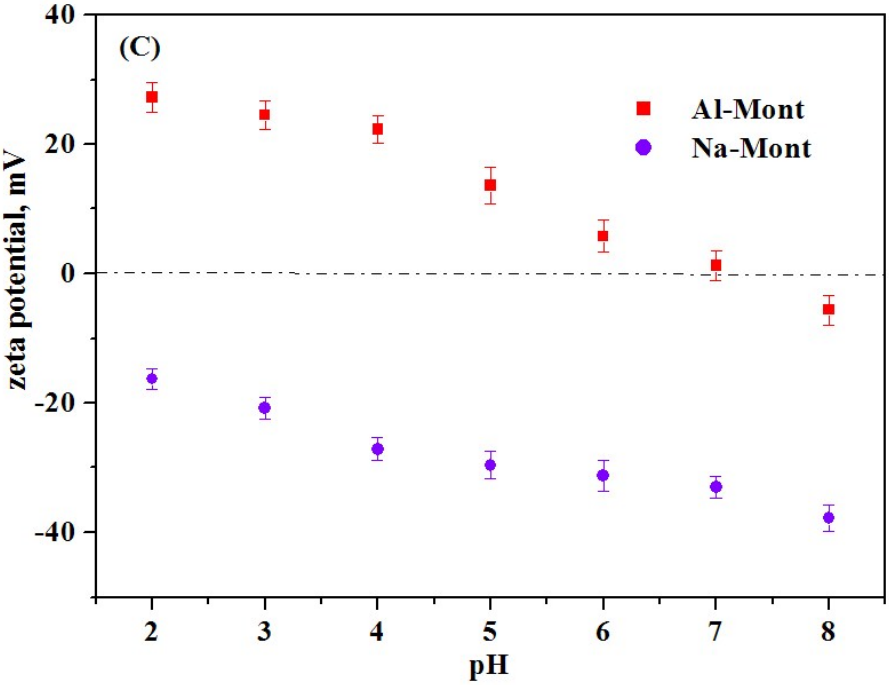

FIGURE S5. The adsorption isotherms of U(VI) (A) and Se(IV) (B) onto Na-Mont, Al-Mont, respectively, and the zeta potentials (C) of Na-Mont and Al-Mont as a function of pH values.

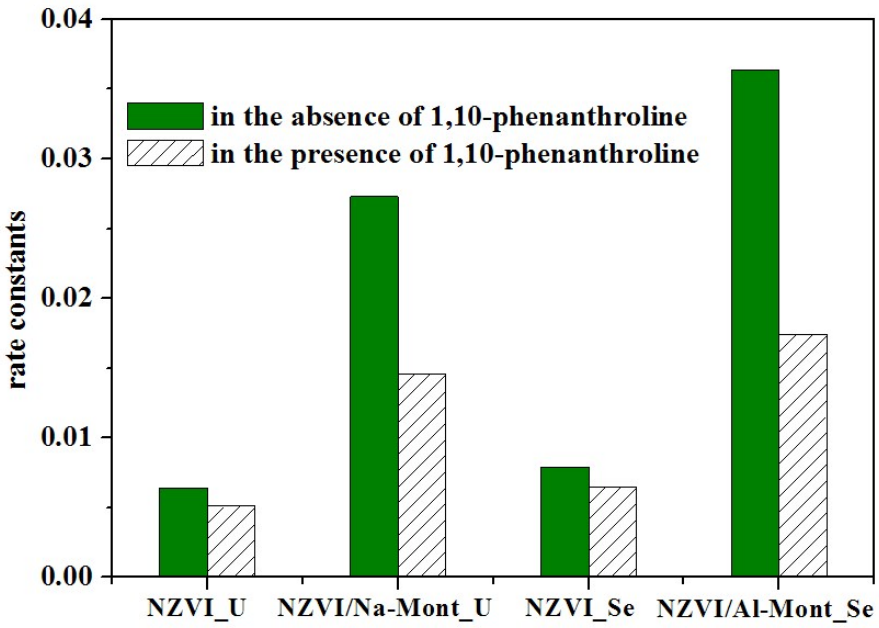

FIGURE S6. The comparison of rate constants for U(VI) and Se(IV) sequestration on iron sources as affected by 1,10-phenanthroline.

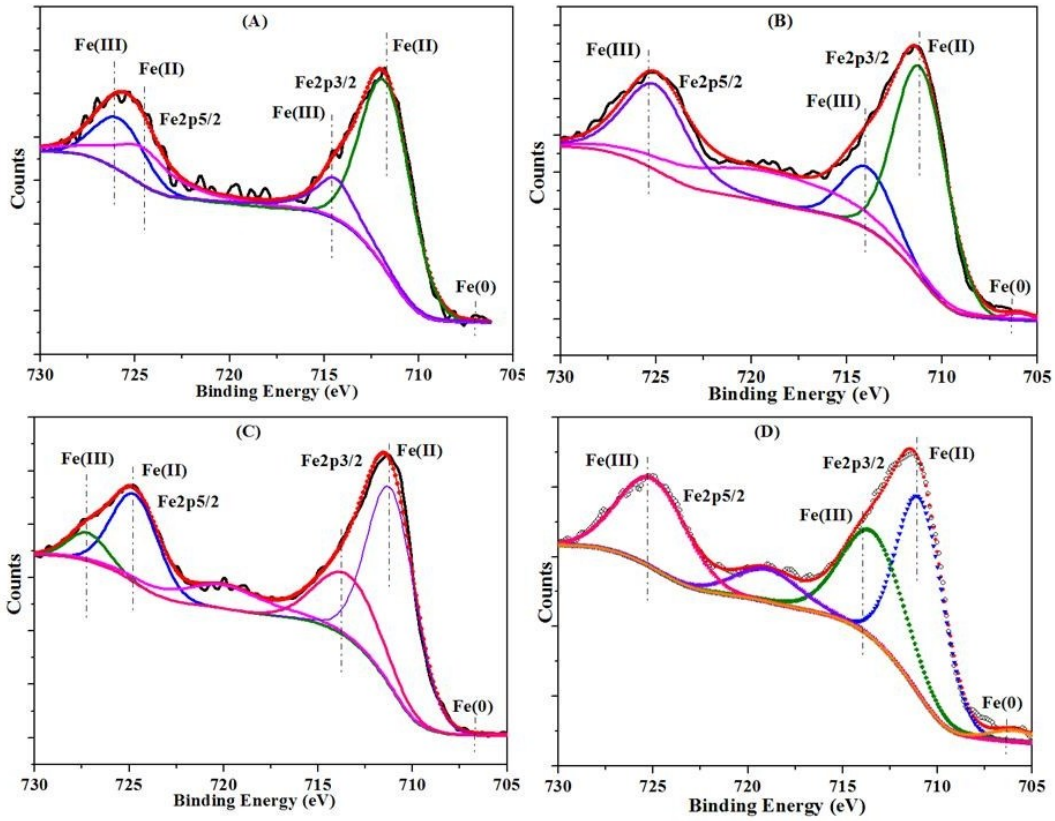

FIGURE S7. The high resolution XPS spectra of Fe2p for NZVI/Na-Mont sample before (A) and after (B) U(VI) sequestration, and for NZVI/Al-Mont sample before (A) and after (B) Se(IV) sequestration.

REFERENCES

[1] Y. Zhang, H. Jiang, Y. Zhang, J. Xie, The dispersity-dependent interaction between montmorillonite supported nZVI and Cr(VI) in aqueous solution. Chemical Engineering Journal 229 (2013) 412–419.

[2] G. Sheng, X. Shao, Y. Li, J. Li, H. Dong, W. Cheng, X. Gao, Y. Huang, Enhanced removal of U(VI) by nanoscale zerovalent iron supported on Na-bentonite and an

investigation of mechanism, J. Phys. Chem. A 118 (2014) 2952–2958.

[3] Y. Li, W. Cheng, G. Sheng, J. Li, H. Dong, Y. Chen, L. Zhu, Synergetic effect of a pillared bentonite support on Se(VI) removal by nanoscale zero valent iron, Appl. Catal. B: Environ. 174–175 (2015) 329–335.

[4] G. Sheng, P. Yang, Y. Tang, Q. Hu, H. Li, X. Ren, B. Hu, X. Wang, Y. Huang, New insights into the primary roles of diatomite in the enhanced sequestration of UO_2^{2+} by zerovalent iron nanoparticles: An advanced approach utilizing XPS and EXAFS. Appl. Catal. B: Environ. 193 (2016) 189–197.

[5] S.M. Webb, SIXPACK: A graphical user interface for XAS analysis using IFEFFIT, Phys. Scr. T 115 (2005) 1011–1014.

[6] M. Newville, IFEFFIT: interactive XAFS analysis and FEFF fitting, J. Synchrotron Rad. 8 (2001) 324–332.

[7] J.J. Rehr, S.I. Zabinsky, R.C. Albers, High-order multiple scattering calculations of X-ray absorption fine structure, Phys. Rev. Lett. 69 (1992) 3397–3400.